Science Advances
AAAS

advances.sciencemag.org/cgi/content/full/6/20/eaay1497/DC1

Supplementary Materials for

Local sympathetic innervations modulate the lung innate immune responses

Tingting Liu, Lu Yang, Xiangli Han, Xiaofan Ding, Jiali Li, Jing Yang*

*Corresponding author. Email: jing.yang@pku.edu.cn

Published 13 May 2020, *Sci. Adv.* **6**, eaay1497 (2020)
DOI: 10.1126/sciadv.aay1497

The PDF file includes:

Other Supplementary Material for this manuscript includes the following:

(available at advances.sciencemag.org/cgi/content/full/6/20/eaay1497/DC1)

Supplementary Movie Legends

Movie S1. Whole-tissue 3D assessment of local neural innervations in the lung.
The intact lung (left lobe) of the adult mouse was processed for the whole-tissue anti-synaptophysin immunolabeling and imaged at 1.26x magnification on the lightsheet microscope. 3D reconstruction of the local neural network in the lung was shown.

Movie S2. Visualization of local neural innervations ensheathing along the airways.
The intact lung (left lobe) of the adult mouse was processed for the whole-tissue anti-synaptophysin immunolabeling and imaged at 12.6x magnification on the lightsheet microscope. The lightsheet scanning and 3D reconstruction of local neural innervations in the 600-μm depth of the tissue were shown.

Movie S3. Whole-tissue 3D assessment of local sympathetic innervations in the lung.
The intact lung (left lobe) of the adult mouse was processed for the whole-tissue anti-TH immunolabeling and imaged at 1.26x magnification on the lightsheet microscope. 3D reconstruction of the local sympathetic network was shown.

Movie S4. Whole-tissue 3D assessment of the inflammatory reaction in the lung.
The wildtype mouse was intranasally treated with chitin. The lung (left lobe) was processed for the whole-tissue anti-Siglec-F immunolabeling and imaged at 1.26x magnification on the lightsheet microscope. 3D reconstruction of the chitin-induced inflammation was shown.

Supplementary Figure Legends

Figure S1. Whole-tissue immunolabeling of the intact lungs of adult mice.

(A to C) Acetone pre-treatment in the iDISCO(ace) procedure preserved the antibody compatibility and the histologic integrity of the lung tissues. The lungs (left lobe) of wildtype mice were untreated or processed through the acetone gradient of the iDISCO(ace) procedure or the methanol gradient of the original iDISCO+. **(A and B)** The tissues were then subjected to 12-μm cryosectioning and immunostained with the indicated antibodies. **(A)** Representative images of anti-PGP9.5, anti-CD3, anti-CD11b, or anti-Siglec-F immunostaining were shown. **(B)** Summary of the antibody compatibility test. The antibodies incompatible with the methanol pre-treatment were highlighted in red. **(C)** The tissues were subjected to 5-μm paraffin-sectioning and assessed by H&E (hematoxylin and eosin) staining. **(D)** Acetone pre-treatment maintained the overall structure of the lung tissues. The lungs (left lobe) of wildtype mice were processed through the iDISCO(ace) procedure. The length, width, and depth of the tissues before and after the procedure were measured. n = 5, n.s., not significant (Student's *t*-test). **(E to H)** Acetone pre-treatment enabled effective antibody penetration through the intact lungs. The lungs (left lobe) of wildtype mice were processed for the whole-tissue immunolabeling of anti-synaptophysin **(E and F)** or anti-TH **(G and H)**. **(E and G)** Representative optical sections at 1.26x magnification of the lightsheet imaging were shown. **(F and H)** Signal-to-background ratios at different locations inside of the tissues were measured. n = 3 for each antibody staining.

Figure S2. Whole-tissue 3D assessment of neural innervations and inflammatory reactions in the intact lungs of adult mice.

(A) Whole-tissue 3D assessment of local neural innervations in the lung. The lung (left lobe) of the adult mouse was processed for the whole-tissue anti-PGP9.5 immunolabeling. Representative 3D-projection image at 1.26x magnification of the lightsheet imaging was shown. **(B)** Whole-tissue 3D assessment of lymphatic vessels in the lung. The wildtype mice were intranasally treated with LPS, and the lungs (left lobe) were then harvested at the indicated time points for the whole-tissue anti-LYVE1 immunolabeling. Representative 3D-projection images at 1.26x magnification of the lightsheet imaging were shown. **(C and D)** Whole-tissue 3D assessment of inflammatory reactions in the lung. The wildtype mice were intranasally treated with papain **(C)** or chitin **(D)**. The lungs (left lobe) were then harvested for the whole-tissue anti-Siglec-F immunolabeling. Representative 3D-projection images at 1.26x magnification of the lightsheet imaging were shown. **(E)** Simultaneous 3D assessment of local sympathetic innervations and the inflammatory reaction in the lung. The wildtype mice were intranasally treated with LPS. The lung (left lobe) was then processed for the whole-tissue co-immunolabeling of anti-TH (green) and anti-F4/80 (red). Representative 3D-projection images of the 600-μm depth of the intact tissue at 12.6x magnification of the lightsheet imaging were shown.

Figure S3. Genetic ablation of local sympathetic innervations in the lung.

(A) Development of sympathetic innervations in the lung. The lungs of the mice at the indicated postnatal ages (P1, P4, and P7: the left and right lobes with the trachea; P14 and

P21: the left lobe with the primary bronchus) were processed for the whole-tissue anti-TH immunolabeling. Representative 3D-projection images at 1.26x magnification of the lightsheet imaging were shown. **(B and C)** The lungs (left lobe) of *Th-Cre; TrkA*$^{+/+}$ and *Th-Cre; TrkA*$^{fl/fl}$ mice were processed for the whole-tissue anti-CGRP immunolabeling. **(B)** Representative 3D-projection images of the 600-μm depth of the intact tissues at 12.6x magnification of the lightsheet imaging were shown. Arrowheads denote the clusters of CGRP-positive neuroendocrine cells. **(C)** CGRP-positive sensory axons were quantified. n = 3, mean ± SEM, n.s., not significant (Student's *t*-test). **(D)** The expression profile of neuronal markers in primary alveolar macrophages was determined by the qPCR analysis. n = 3, mean ± SEM.

Figure S4. Pharmacologic or surgical ablation of local sympathetic innervations in the lung.

(A to G) The wildtype mice were intranasally treated with saline control or 6-OHDA. **(A and B)** The lungs (left lobe) of saline-treated and 6-OHDA-treated mice were processed for the whole-tissue anti-VChAT immunolabeling. **(A)** Representative 3D-projection images of the 600-μm depth of the intact tissues at 12.6x magnification of the lightsheet imaging were shown. **(B)** VChAT-positive parasympathetic axons were quantified. n = 4, mean ± SEM, n.s., not significant (Student's *t*-test). **(C to G)** The femurs **(C)**, spleens **(D)**, thymuses **(E)**, and subcutaneous lymph nodes **(F)** of saline-treated and 6-OHDA-treated mice were processed for the whole-tissue anti-TH immunolabeling (Femurs: BoneClear method as reported; Spleens, thymuses, and lymph nodes: ImmuView method as reported) **(C to F)** Representative 3D-projection images at 1.26x magnification of the

lightsheet imaging were shown. **(G)** TH-positive sympathetic axons in each tissue type were quantified. n = 3, mean ± SEM, n.s., not significant (Student's *t*-test). **(H and I)** The wildtype mice were subjected to the local sympathectomy of the lung. The femurs, spleens, thymuses, and subcutaneous lymph nodes of the mice after mock surgery or sympathectomy were processed for the whole-tissue anti-TH immunolabeling. **(H)** Representative 3D-projection images of the thymuses at 1.26x magnification of the lightsheet imaging were shown. **(I)** TH-positive sympathetic axons in each tissue type were quantified. n = 3, mean ± SEM, n.s., not significant (Student's *t*-test).

Figure S5. Local sympathetic innervations negatively modulate the innate immune responses in the lung.

(A and B) Genetic ablation of local sympathetic innervations enhanced the IL-33-elicited type 2 innate immunity in the lung. *Th-Cre; TrkA*$^{+/+}$ and *Th-Cre; TrkA*$^{fl/fl}$ mice were intranasally treated with saline control or IL-33. The lungs were harvested at 24 hr after the 2nd instillation. **(A)** CD45^{+} CD11c^{-} Siglec-F^{+} eosinophils were examined by the FACS analysis. **(B)** Expression levels of cytokines were determined by the qPCR analysis. n = 5, mean ± SEM, * $p < 0.01$ (ANOVA test). **(C)** Pharmacologic ablation of local sympathetic innervations promoted the IL-33-elicited immune response in the lung. The wildtype mice were intranasally treated with saline control or 6-OHDA and then intranasally administered with IL-33. The lungs were harvested at 24 hr after the 2nd instillation and assessed by H&E staining. The histologic scores were determined. n = 3, mean ± SEM, * $p < 0.01$ (ANOVA test). **(D to F)** CXCL2 mediated the LPS-elicited recruitment of Ly-6G^{+} neutrophils in the lung. 6-OHDA-treated wildtype mice **(D and E)**

or *Adrb2*$^{-/-}$ mice **(F)** were intravenously injected with control IgG or anti-CXCL2. The mice were then intranasally administered with LPS, and the lungs (left lobe) were processed for the whole-tissue anti-Ly-6G immunolabeling. **(D)** Representative 3D-projection images at 1.26x magnification of the lightsheet imaging were shown. **(E and F)** The density of Ly-6G^{+} neutrophils was quantified. n = 4, mean ± SEM, * $p < 0.01$ (Student's *t*-test).

Figure S6. β2-adrenergic receptor signaling inhibits the innate immune responses in the lung.

(A and B) *Adrb2*$^{+/+}$ and *Adrb2*$^{-/-}$ mice were intranasally treated with saline control or LPS. Alveolar macrophages (CD45^{+} CD11c^{+} Siglec-F^{+}) and interstitial macrophages (CD45^{+} CD11c^{-} Siglec-F^{-} F4/80^{+}) in the lungs were quantified by the FACS analysis. n = 4, mean ± SEM, n.s., not significant (ANOVA test). **(C to F)** Pharmacologic inhibition of the β2-adrenergic receptor enhanced the innate immune responses in the lung. The wildtype mice were intranasally treated LPS **(C and D)** or IL-33 **(E and F)** in combination with saline control or ICI-118,551. The lungs (left lobe) were processed for the whole-tissue immunolabeling of anti-Ly-6G or anti-Siglec-F. **(C and E)** Representative 3D-projection images at 1.26x magnification of the lightsheet imaging were shown. **(D)** The density of Ly-6G^{+} neutrophils was quantified. n = 4, mean ± SEM, * $p < 0.01$ (ANOVA test). **(F)** The density of Siglec-F^{+} immune cells was quantified. n = 4, mean ± SEM, * $p < 0.01$ (ANOVA test).

Figure S1

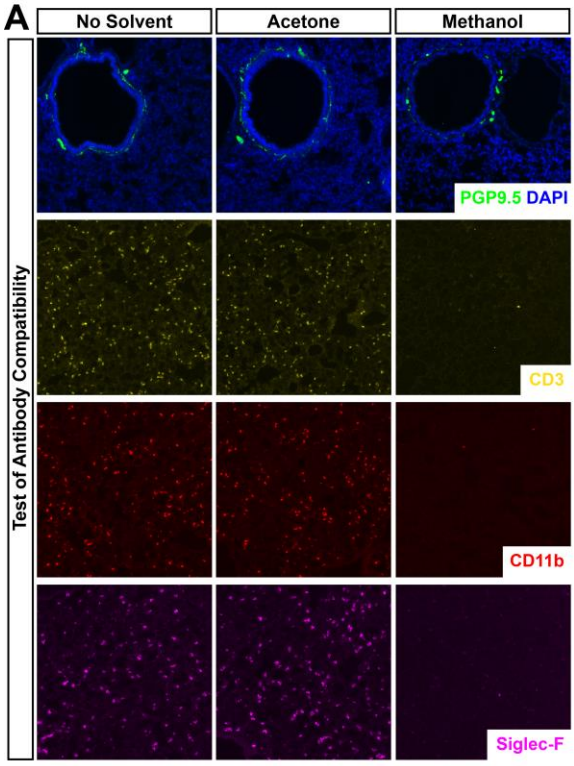

B

	No Solvent Pretreatment	Acetone Pretreatment	Methanol Pretreatment
anti-Synaptophysin	Yes	Yes	Yes
anti-Tuj1	Yes	Yes	No
anti-PGP9.5	Yes	Yes	Yes
anti-TH	Yes	Yes	Yes
anti-VChAT	Yes	Yes	Yes
anti-CGRP	Yes	Yes	Yes
anti-Cytokeratin	Yes	Yes	Yes
anti-LYVE1	Yes	Yes	No
anti-PECAM1	Yes	Yes	Yes
anti-CD3	Yes	Yes	No
anti-CD4	Yes	Yes	No
anti-CD8	Yes	Yes	No
anti-CD11b	Yes	Yes	No
anti-CD11c	Yes	Yes	No
anti-CD19	Yes	Yes	No
anti-CD45R	Yes	Yes	No
anti-NK1.1	Yes	Yes	No
anti-Ly-6G	Yes	Yes	No
anti-F4/80	Yes	Yes	No
anti-Siglec-F	Yes	Yes	No
anti-Ki67	Yes	Yes	Yes
anti-GFP	Yes	Yes	Yes
anti-DsRed	Yes	Yes	Yes
anti-mCherry	Yes	Yes	Yes

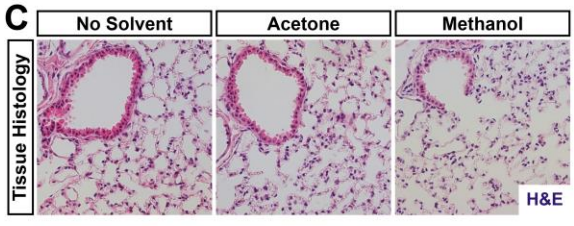

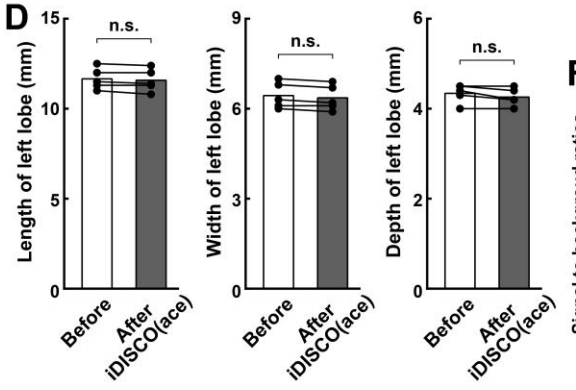

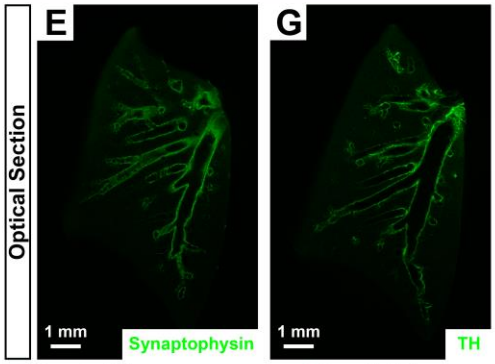

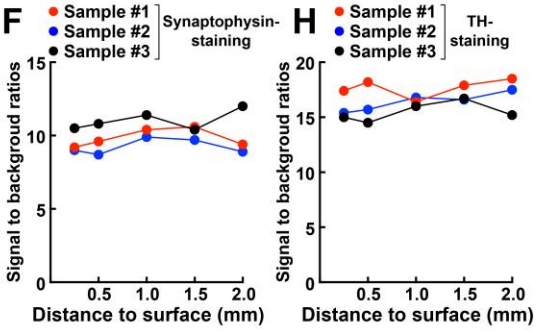

Figure S2

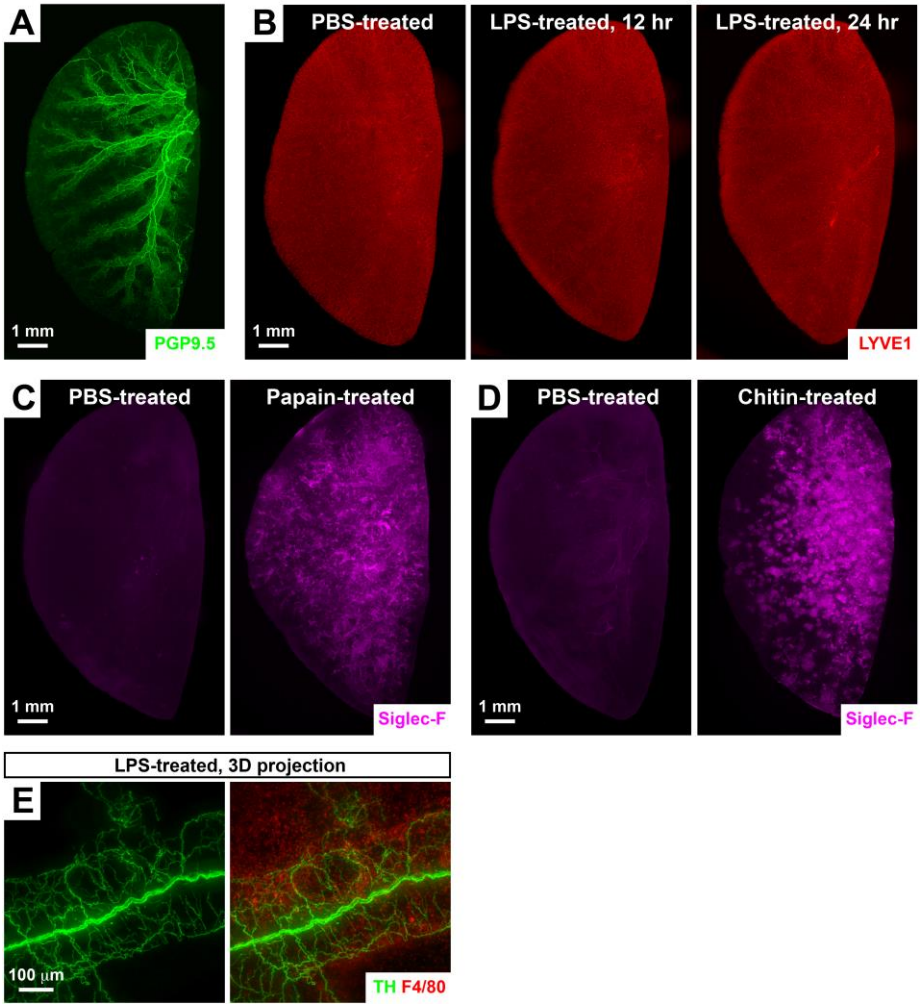
A
1 mm
PGP9.5
B
PBS-treated
1 mm
LPS-treated, 12 hr
LPS-treated, 24 hr
LYVE1
C
PBS-treated
1 mm
Papain-treated
Siglec-F
D
PBS-treated
1 mm
Chitin-treated
Siglec-F
LPS-treated, 3D projection
E
100 μm
TH F4/80

Figure S3

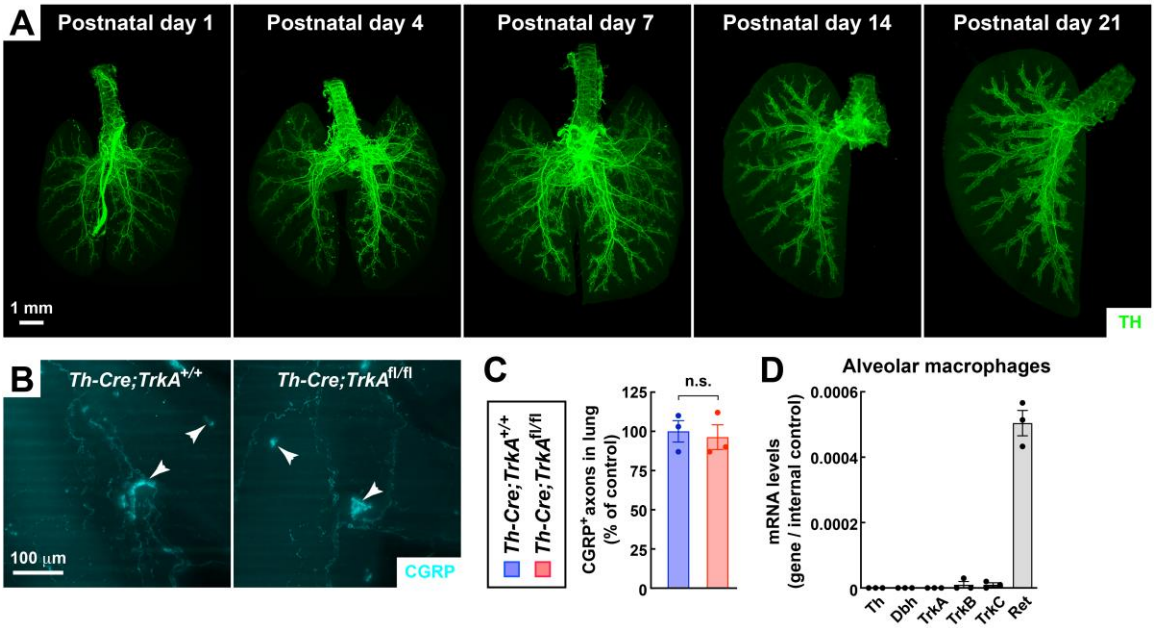
A
Postnatal day 1
Postnatal day 4
Postnatal day 7
Postnatal day 14
Postnatal day 21
1 mm
TH
B
Th-Cre;TrkA+/+
Th-Cre;TrkAfl/fl
100 μm
CGRP
C
Th-Cre;TrkA+/+
Th-Cre;TrkAfl/fl
CGRP+ axons in lung (% of control)
n.s.
125
100
75
50
25
0
D
Alveolar macrophages
mRNA levels (gene / internal control)
0.0006
0.0004
0.0002
0
Th
Dbh
TrkA
TrkB
TrkC
Ret

Figure S4

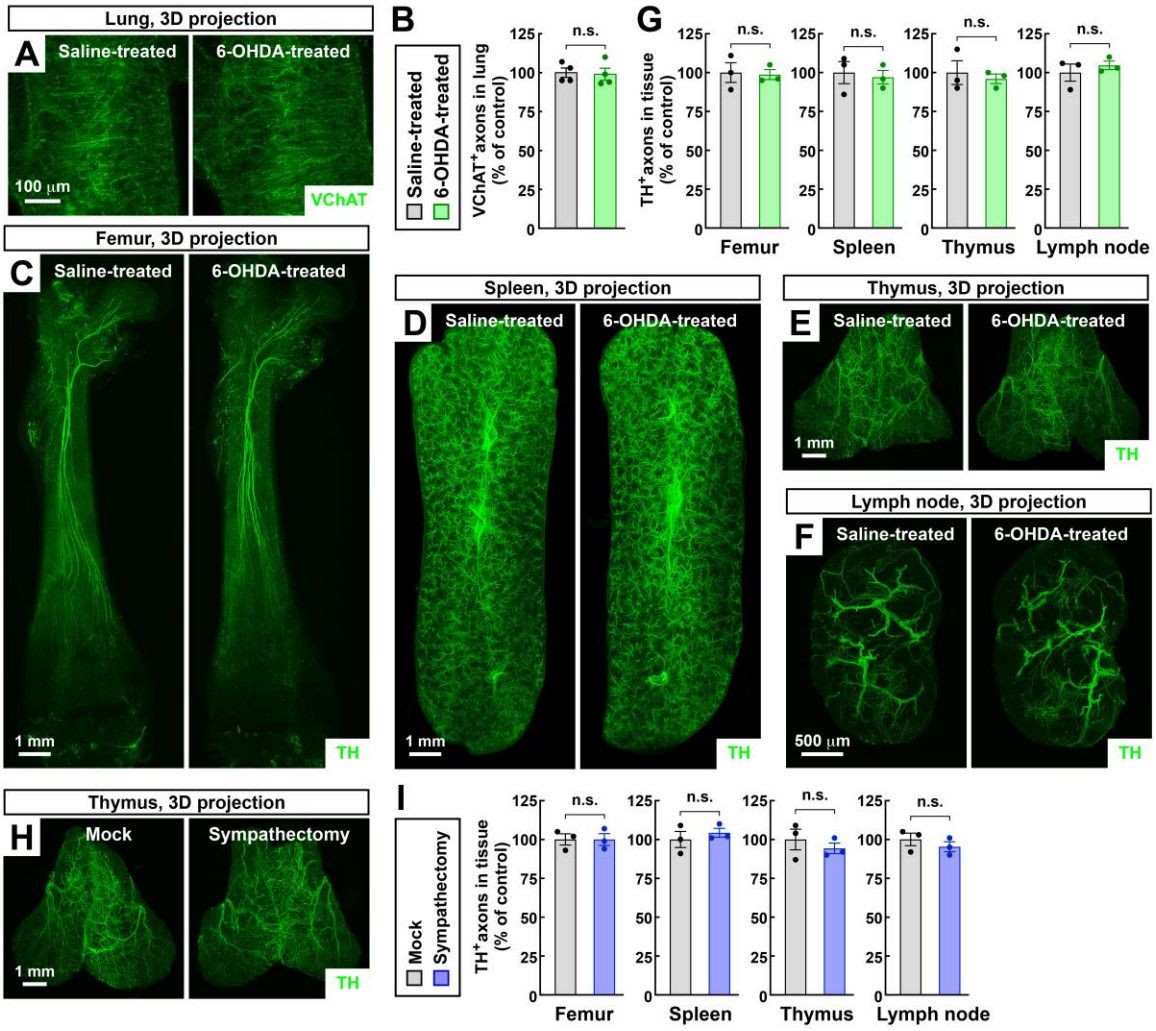
Lung, 3D projection
A
Saline-treated
6-OHDA-treated
100 μm
VChAT
B
Saline-treated
6-OHDA-treated
VChAT+ axons in lung (% of control)
n.s.
G
TH+ axons in tissue (% of control)
n.s.
Femur
Spleen
Thymus
Lymph node
Femur, 3D projection
C
Saline-treated
6-OHDA-treated
1 mm
TH
Spleen, 3D projection
D
Saline-treated
6-OHDA-treated
1 mm
TH
Thymus, 3D projection
E
Saline-treated
6-OHDA-treated
1 mm
TH
Lymph node, 3D projection
F
Saline-treated
6-OHDA-treated
500 μm
TH
Thymus, 3D projection
H
Mock
Sympathectomy
1 mm
TH
I
Mock
Sympathectomy
TH+ axons in tissue (% of control)
n.s.
Femur
Spleen
Thymus
Lymph node

Figure S5

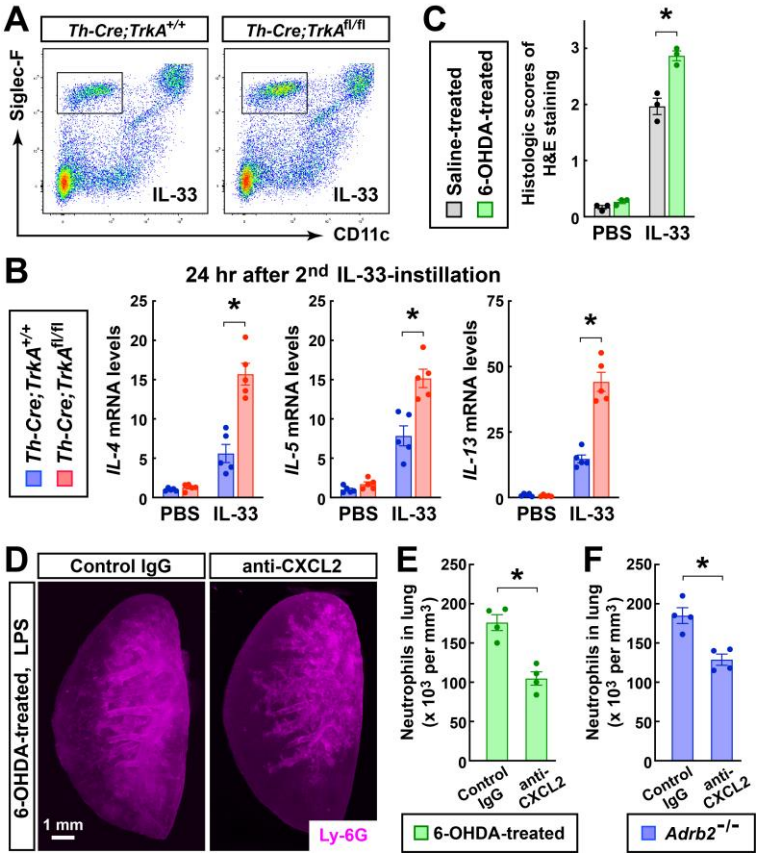
A
Th-Cre;TrkA+/+
Th-Cre;TrkAfl/fl
Siglec-F
CD11c
IL-33
IL-33
C
Saline-treated
6-OHDA-treated
Histologic scores of H&E staining
PBS
IL-33
B
24 hr after 2nd IL-33-instillation
Th-Cre;TrkA+/+
Th-Cre;TrkAfl/fl
IL-4 mRNA levels
IL-5 mRNA levels
IL-13 mRNA levels
PBS
IL-33
D
Control IgG
anti-CXCL2
6-OHDA-treated, LPS
1 mm
Ly-6G
E
Neutrophils in lung (x 10³ per mm³)
Control IgG
anti-CXCL2
6-OHDA-treated
F
Neutrophils in lung (x 10³ per mm³)
Control IgG
anti-CXCL2
Adrb2−/−

Figure S6

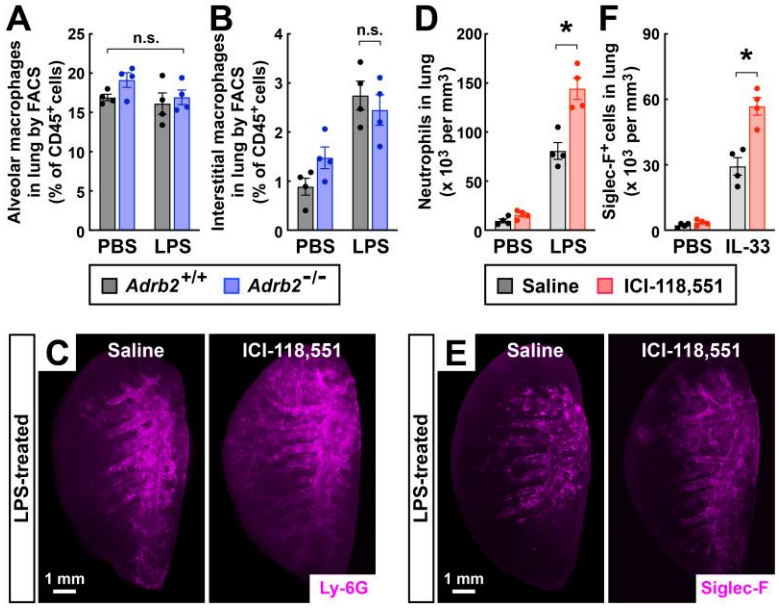
A
Alveolar macrophages in lung by FACS (% of CD45+ cells)
n.s.
PBS
LPS
B
Interstitial macrophages in lung by FACS (% of CD45+ cells)
n.s.
PBS
LPS
Adrb2+/+
Adrb2-/-
D
Neutrophils in lung (x 10³ per mm³)
*
PBS
LPS
F
Siglec-F+ cells in lung (x 10³ per mm³)
*
PBS
IL-33
Saline
ICI-118,551
C
Saline
ICI-118,551
LPS-treated
1 mm
Ly-6G
E
Saline
ICI-118,551
LPS-treated
1 mm
Siglec-F